Support information

Triplet-Triplet Annihilation Upconversion with Reversible Emission-Tunability Induced by Chemical-Stimuli: a Remote Modulator for Photocontrol Isomerization

Yaxiong Wei,[a,b] Haitao Xian,[a] Xialei Lv,[a,b] Fan Ni,[a,b] Xiaosong Cao,[a]* and Chuluo Yang[a]*

[a] Shenzhen Key Laboratory of Polymer Science and Technology, College of Materials Science and Engineering, Shenzhen University, Shenzhen 518060, China. E-mail: xcao@szu.edu.cn; clyang@szu.edu.cn

[b] College of Physics and Optoelectronic Engineering, Shenzhen University, Shenzhen 518060, China

Contents

1. Experimental instruments and measurement processes

1.1. Commercial instruments. ^{1}H NMR spectra were recorded with a 500 MHz spectrophotometer (AVANCE III 500, Bruker), where $CDCl_3$ was used as solvent and tetramethylsilane (TMS) was applied as an internal standard for which $\delta = 0.00$ ppm. Steady-state UV-Vis absorption spectra were recorded in a wavelength range of 300-800 nm with a spectrophotometer (UV-2600, Shimadzu). Fluorescence emission spectra were measured with a fluorescence spectrophotometer (F-7100, Hitachi) in a wavelength range of 400−800 nm. The transient PL decay curves were obtained by FluoTime 300 (PicoQuant GmbH) with a Picosecond Pulsed UV-LASTER (LASTER375) as the excitation source. The fluorescence quantum yields were measured on a Hamamatsu UV-NIR absolute PL quantum yield spectrometer (C13534, Hamamatsu Photonics) equipped with a calibrated integrating sphere, the integrating sphere was purged with dry argon to maintain an inert atmoshphere, all the samples were excited at 390 nm.

1.2. TTA-UC spectra. TTA-UC spectra were recorded using a modified fluorescence spectrometer (F-7100, Hitachi). A few semiconductor lasers with 638 nm was selected as the excitation light source. The diameter of the laser spot in sample cell region was ~5 mm. In the TTA-UC experiments, the solutions mixing photosensitizer and acceptor were kept in a quartz cuvette (10 mm × 10 mm), deoxygenated by purging with high-purity Argon for 15 minutes. In experiments, the upconverted fluorescence of acceptors was collected and detected with a commercial fluorescence spectrometer (F-7100, Hitachi), under photoexcitation at 638 nm.

1.3. Density functional theory calculations. Geometries of the compounds were optimized using density functional theory (DFT) with the B3LYP function and 6-31G(d) basis set. No imaginary frequencies were confirmed for all the optimized structures. The spin density surfaces of the complexes, and the energy gaps between ground state and lowest triplet state were calculated with time-dependent DFT (TD-DFT) level using the same basis set. The vertical excitation energies were directly compared with absorption spectra, and the corresponding electronic transitions were

identified subsequently. The PCM model was applied to evaluate the solvent effect. All these calculations were performed with the Gaussian 09W program package.

1.4. TTET efficiency. In the presence of triplet acceptor, a bimolecular TTET process could occur between the triplet dyad and the acceptor. The corresponding efficiency, Φ_{TTET}, can be determined as equation (S1), without taking into account the weak phosphorescence emission.

$$\Phi_{TTET} = \frac{k_{TTET}\cdot[acceptor]}{k_{TTET}\cdot[acceptor] + k_{NR}} = \frac{1/\tau - 1/\tau_T}{1/\tau} \quad \text{(S1)}$$

where k_{NR} is the overall rate constant of non-radiation processes such as collision and internal conversion, and k_{TTET} is the quenching rate constant of the triplet photosensitizer by the acceptor. Actually, k_{NR} can be determined as $k_{NR}=1/\tau_T$, and $k_{TTET}\cdot[acceptor]$ is expressed by $(1/\tau - 1/\tau_T)$, where τ_T and τ are the lifetimes of the triplet photosensitizer in the absence and presence of acceptor, respectively.

1.5. TTA-UC quantum yields. In this experiment, using the upconversion emission of $Os(phen)_3^{2+}$/DPA system as the standard (Φ_{std} = 5.9% in dichloroethane),[1] the TTA-UC quantum yields, Φ_{UC}, could be determined by equation (S2).

$$\Phi_{UC} = \Phi_{std}\cdot\left(\frac{A_{std}}{I_{std}}\right)\cdot\left(\frac{I_{sam}}{A_{sam}}\right)\cdot\left(\frac{\eta_{sam}}{\eta_{std}}\right)^2 \quad \text{(S2)}$$

where A, I, and η are the absorbance intensity, the integrated emission intensity, and the refractive index of the solvents used for standard and samples.

2. Synthesis of Os(II) complex and acceptor

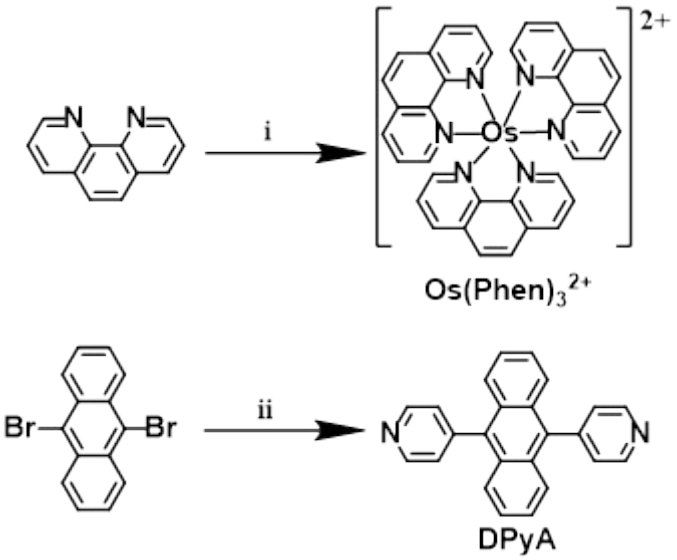

Scheme S1. Synthesis route of the photosensitizer and acceptor. Reaction conditions: (i) $K_2[OsCl_6]$, ethylene glycol, reflux, 10h; $NH_4{\cdot}PF_6$, room temperature, 1h; (ii) 4-pyridylboronic acid, $Pd(PPh_3)_4$, K_2CO_3, DMF/H_2O = 6/1 (*v*/*v*), 120℃, 24 h.

The specific synthesis steps of $Os(phen)_3^{2+}$ are described in detail in our previous works.[1, 2]

DPyA: To a dry two-necked round-bottom flask was added 9,10-dibromoanthracene (3 g, 8.9 mmol), 4-pyridylboronic acid (2.6 g, 21 mmol), potassium carbonate (6.9 g, 50 mmol) and $Pd(PPh_3)_4$ (115 mg, 0.1 mmol) in sequence. DMF/H_2O (6/1, *v*/*v*, 120/20 ml) were subsequently added to the flask and the solution was degassed with argon for 25 min. The reaction solution was heated at 120ºC under argon for 24 h. The cooled reaction solution was poured into water and extracted with CH_2Cl_2 for three times(3×150 mL). After removal of the solvent under reduced pressure, the residual solid was purified via column chromatography (silica gel. CH_2Cl_2/PE/TEA = 100/100/2, *v*/*v*/*v*). The product was obtained as a light yellow solid (2.0 g, 68 %). ^{1}H NMR (500 MHz, $CDCl_3$) δ 8.88 (d, *J* = 4.4, 1.5 Hz, 4H), 7.61 (dd, *J* = 6.8, 3.3 Hz, 4H), 7.45 (dd, *J* = 4.3, 1.6 Hz, 4H), 7.40 (dd, *J* = 6.9, 3.2 Hz, 4H), 1.82 (s, 2H). ^{13}C NMR (125 MHz, $CDCl_3$) δ 150.1, 147.4, 134.7, 129.0, 126.4, 126.3, 125.9.

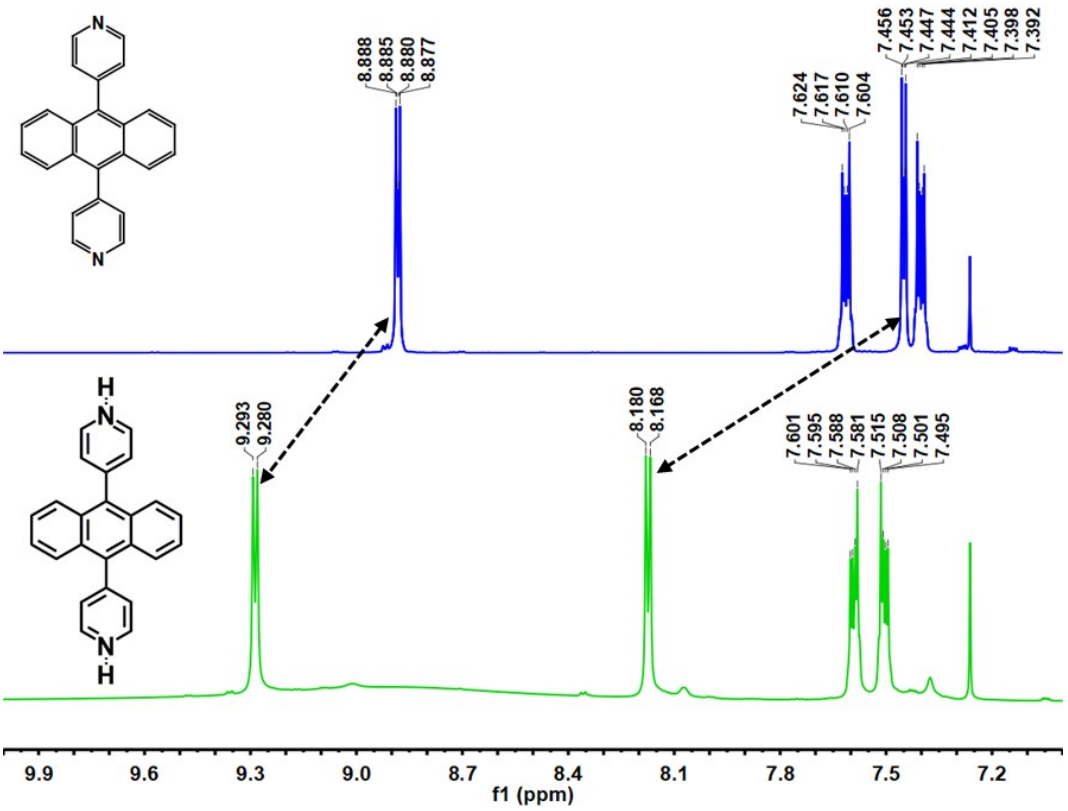

Figure S1. ^{1}H NMR of DPyA and P-DPyA in $CDCl_3$ (500 MHz).

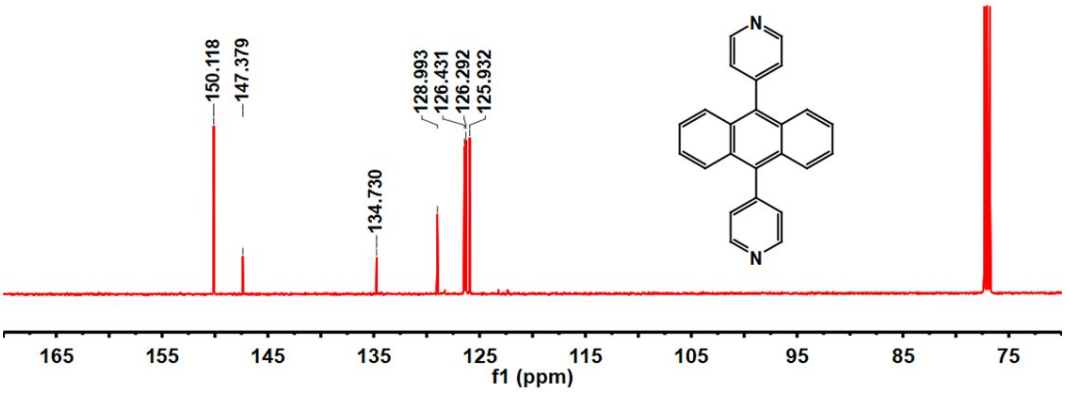

Figure S2. ^{13}C NMR of DPyA in $CDCl_3$ (125 MHz).

3. The steady-state and transient-state spectra

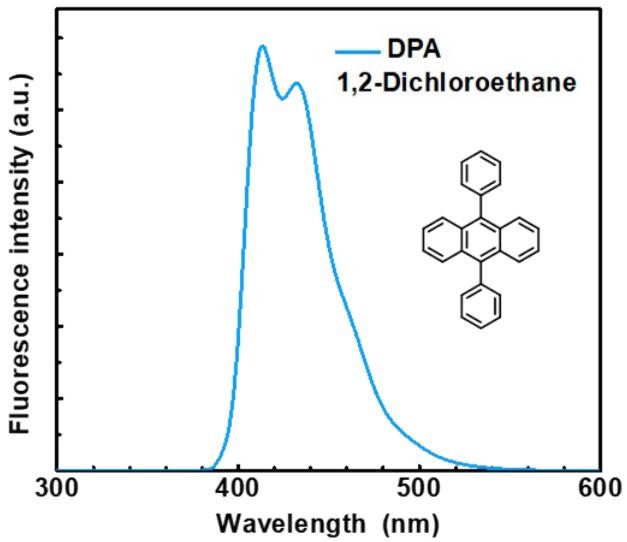

Figure S3. The fluorenscence emission spectrum of DPA under photoexcitation at 390 nm, c[DPyA] = 1×10^{-5} M, 1,2-dichloroethane as solvent.

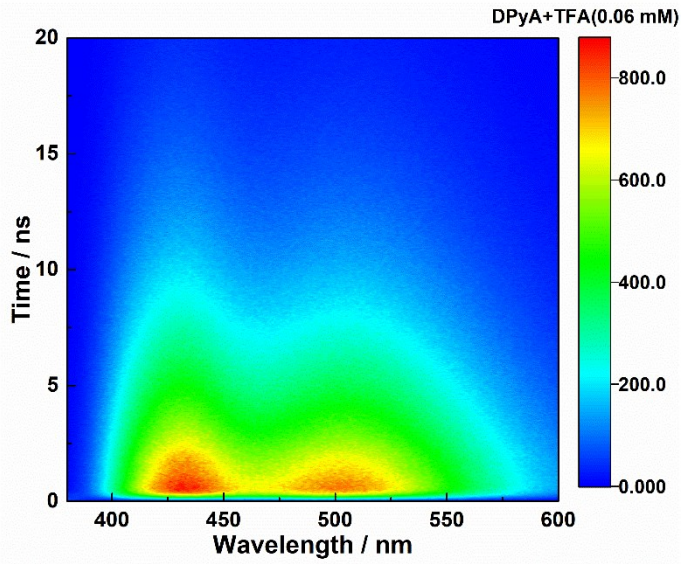

Figure S4. The time-resolved emission spectrum of DPyA in the presence of 0.06 mM TFA. c[DPyA]= 1×10^{-5} M, 1,2-dichloroethane as solvent.

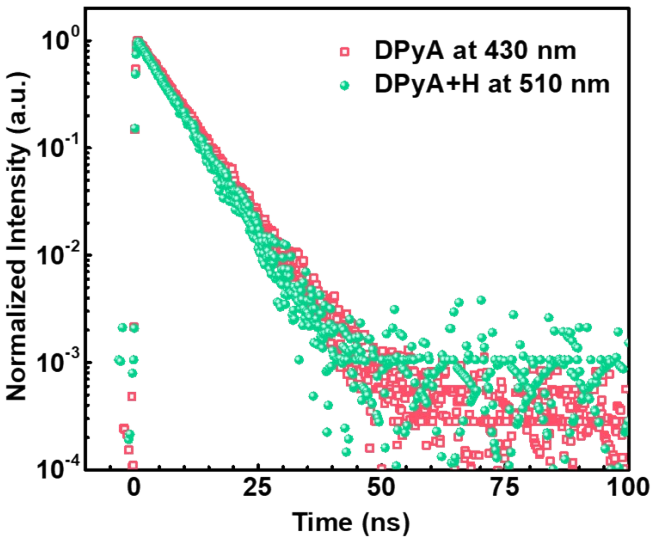

Figure S5. The transient photoluminescence decay curves of DPyA and P-DPyA, λ_{ex} = 375 nm. c[DPyA] or c[P-DPyA]= 1×10^{-5} M, 1,2-dichloroethane as solvent.

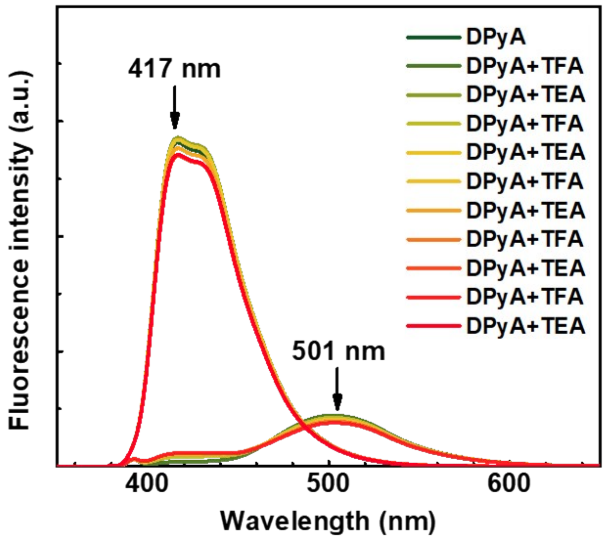

Figure S6. The reversibility of acid-base switching of fluorescence with DPyA upon excitation with 390 nm light. Trifluoroacetic acid (TFA) as acid, triethylamine (TEA) as base.

4. DFT calculations results

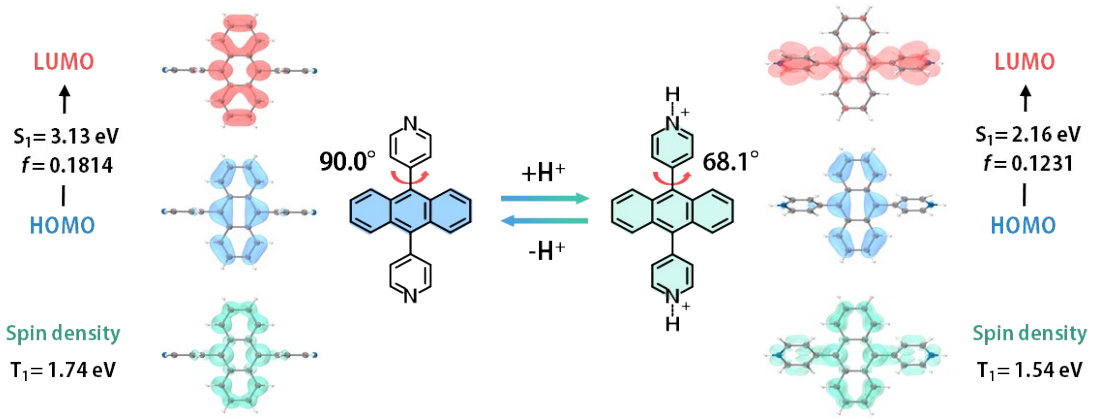

Figure S7. DFT calculation results, singlet and triplet state energy levels, frontier molecular orbitals, spin density surfaces of DPyA and P-DPyA.

The optimized ground state geometry of DPyA

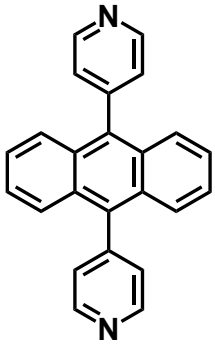

N	5.74958700	0.00000200	0.00000000
C	5.04629100	0.00051300	-1.14065600
C	3.65218300	0.00052400	-1.19538700
C	2.92155900	-0.00000100	0.00000000
C	3.65218300	-0.00052500	1.19538700
C	5.04629200	-0.00051300	1.14065600
C	1.42470600	-0.00000200	0.00000000
C	0.72331800	-1.22469300	-0.00002500
C	-0.72332100	-1.22469200	0.00002600
C	-1.42470600	0.00000000	0.00000000
C	-0.72331800	1.22469000	-0.00002600
C	0.72332100	1.22468900	0.00002600
C	-1.40247800	2.48664100	-0.00011900
C	-0.71132800	3.66898500	-0.00007600
C	0.71133700	3.66898300	0.00007500
C	1.40248400	2.48663700	0.00011800
C	1.40247800	-2.48664400	-0.00011800
C	0.71132900	-3.66898800	-0.00007500
C	-0.71133700	-3.66898600	0.00007600
C	-1.40248400	-2.48664000	0.00011900
C	-2.92156000	0.00000200	0.00000000
C	-3.65218400	0.00052900	1.19538700
C	-5.04629200	0.00051900	1.14065600
N	-5.74958700	0.00000400	0.00000000
C	-5.04629200	-0.00051000	-1.14065600

C	-3.65218400	-0.00052400	-1.19538700
H	5.62708500	0.00091500	-2.06171200
H	3.14214200	0.00094100	-2.15409600
H	3.14214200	-0.00094000	2.15409600
H	5.62708600	-0.00091100	2.06171200
H	-2.48688800	2.49495200	-0.00023200
H	-1.24950500	4.61276400	-0.00015600
H	1.24951600	4.61276000	0.00015400
H	2.48689400	2.49494600	0.00023100
H	2.48688800	-2.49495600	-0.00023100
H	1.24950500	-4.61276700	-0.00015400
H	-1.24951600	-4.61276400	0.00015500
H	-2.48689300	-2.49494900	0.00023200
H	-3.14214200	0.00094500	2.15409600
H	-5.62708600	0.00091900	2.06171200
H	-5.62708600	-0.00091300	-2.06171200
H	-3.14214200	-0.00094200	-2.15409600

The optimized ground state geometry of P-DPyA

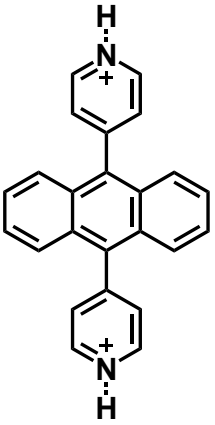

N	-5.66235400	0.00016700	-0.00202000
C	-5.01363700	-0.44522300	-1.10028600
C	-3.63200600	-0.45703000	-1.11700200
C	-2.90709600	-0.00024600	0.00019500
C	-3.63362400	0.45643800	1.11634900
C	-5.01526600	0.44509600	1.09737500
C	-1.41651900	-0.00012800	0.00088400
C	-0.72349700	1.23283500	-0.00600800
C	0.72331900	1.23289200	0.00778400
C	1.41651000	0.00005000	0.00072400
C	0.72349800	-1.23291600	-0.00609800
C	-0.72331000	-1.23298000	0.00788800
C	1.39938200	-2.49466700	-0.05166100
C	0.70951600	-3.67764400	-0.03311800
C	-0.70918500	-3.67770800	0.03493700
C	-1.39911800	-2.49477300	0.05346400
C	-1.39937400	2.49459800	-0.05151200
C	-0.70950600	3.67757100	-0.03305400
C	0.70921000	3.67761200	0.03478700
C	1.39914200	2.49467900	0.05321500
C	2.90709500	0.00018600	-0.00000800
C	3.63352200	-0.45633300	1.11631500
C	5.01514900	-0.44479200	1.09757400
N	5.66232900	0.00010500	-0.00181100

C	5.01373800	0.44520800	-1.10021600
C	3.63208200	0.45688800	-1.11713700
H	-5.62756700	-0.77154000	-1.93033200
H	-3.11908900	-0.81179100	-2.00315400
H	-3.12208600	0.81092300	2.00341600
H	-5.63045400	0.77155300	1.92644800
H	2.48147400	-2.51670700	-0.10998200
H	1.24649200	-4.62020200	-0.06791500
H	-1.24608500	-4.62030600	0.06977500
H	-2.48120500	-2.51679400	0.11188200
H	-2.48147100	2.51659500	-0.10973900
H	-1.24647600	4.62013300	-0.06776100
H	1.24612600	4.62020700	0.06951200
H	2.48124400	2.51673600	0.11140200
H	3.12183800	-0.81077800	2.00331000
H	5.63028900	-0.77111400	1.92673400
H	5.62774700	0.77155900	-1.93019700
H	3.11927400	0.81148500	-2.00341700
H	-6.67980700	0.00058000	-0.00294800
H	6.67979000	-0.00011800	-0.00256500

5. TTA-UC spectrum with TFA and TEA

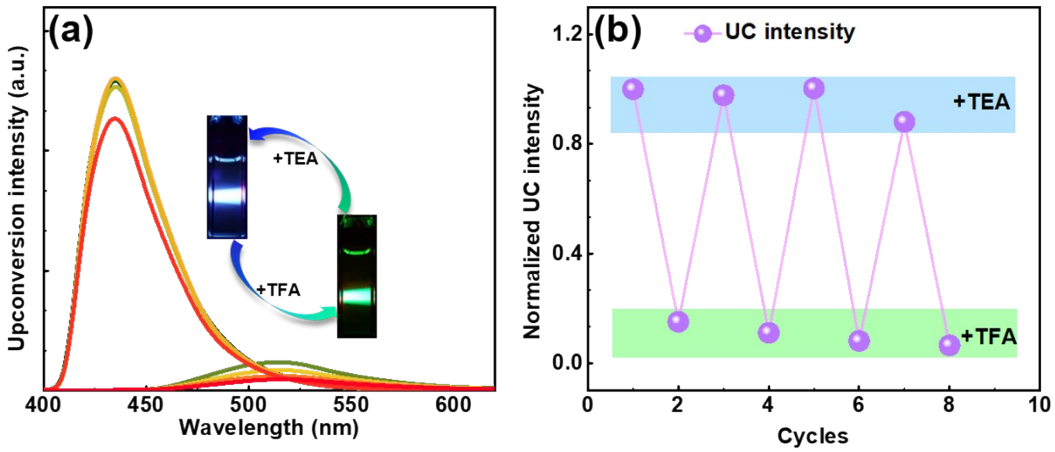

Figure S8. (a) The reversibility of acid-base (TFA-TEA) induced TTA-UC emission switching of $Os(phen)_3^{2+}$/DPyA system with a shortpass filter at 635 nm. (b) The reversibility of the acid-base switching of UC emission intensity. 1,2-Dichloroethane as the solvent, c[$Os(phen)_3^{2+}$] = 1×10^{-5} M, c[DPyA]=5 mM, λ_{ex} = 638 nm.

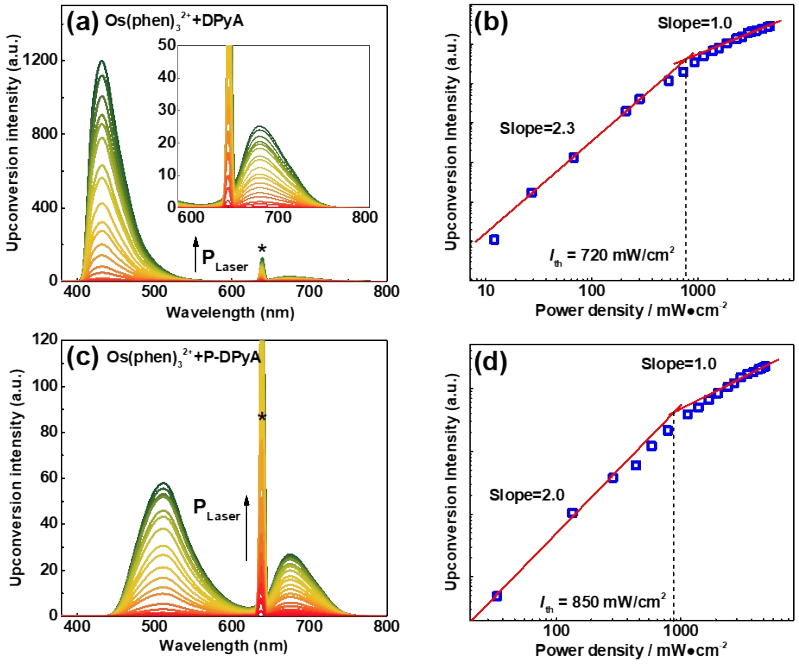

Figure S9. (a, c) Dependence of the upconverted fluorescence intensity on the excitation power density with the DPyA and P-DPyA as acceptors, respectively; (b, d) A double logarithmic plot of integrated TTA upconversion fluorescence intensity with excitation power density. c[$Os(phen)_3^{2+}$] = 1×10^{-5} M, c[DPyA]=5 mM, λ_{ex} = 638 nm.

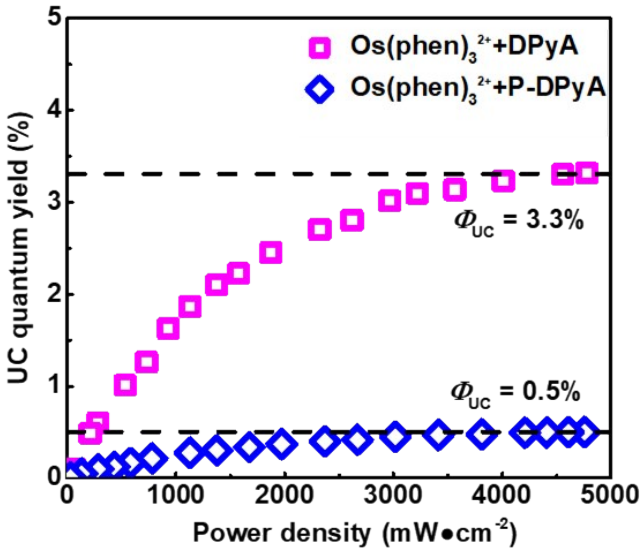

Figure S10. Dependence of the TTA-UC quantum yield on the excitation power density, c[$Os(phen)_3^{2+}$] = 1×10^{-5} M, c[DPyA]=5 mM, λ_{ex} = 638 nm.

6. The TTA-UC delay fluorescence

The TTA-UC delay fluorescence shows exponential decay, can be fitted by the equation S3

$$I_{UC}(t) \propto exp(-t/\tau_{UC}) = exp(-2t/\tau_T) \quad \text{(S3)}$$

Where the τ_{UC} and τ_T are lifetime of the UC emission and acceptor triplet, respectively.

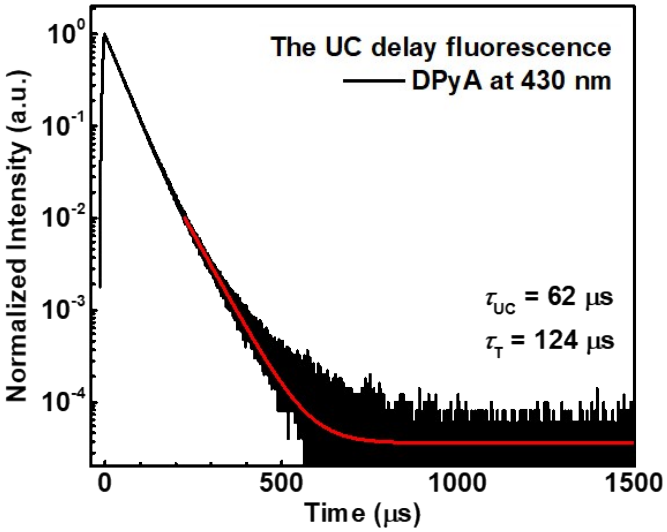

Figure S11. TTA-UC delay fluorescence of $Os(phen)_3^{2+}$ and DPyA in deaerated 1,2-dichloroethane under excitation at 640 nm. c[$Os(phen)_3^{2+}$] = 0.01 mM, c[DPyA] = 5 mM.

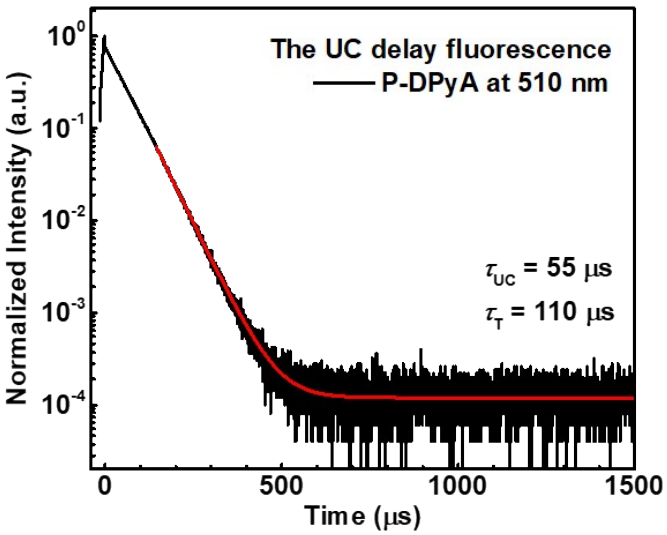

Figure S12. TTA-UC delay fluorescence of $Os(phen)_3^{2+}$ and P-DPyA in deaerated 1,2-dichloroethane under excitation at 640 nm. c[$Os(phen)_3^{2+}$] = 0.01 mM, c[P-DPyA] = 5 mM.

7. The stability of photosensitizer in the presence of TFA

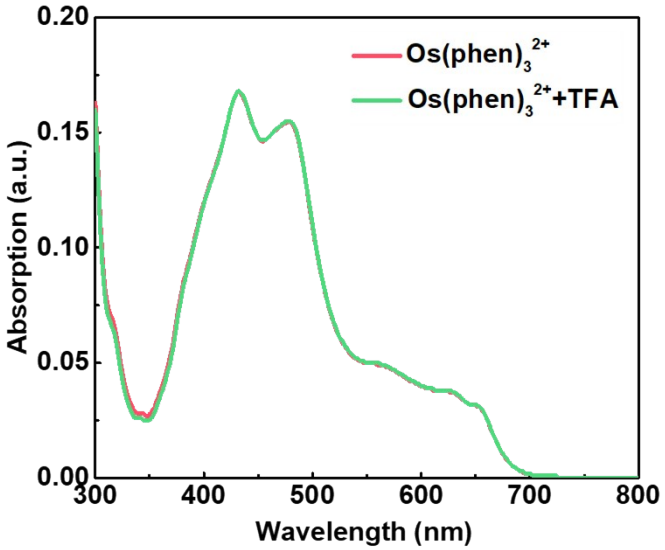

Figure S13. The absorption spectra of $Os(phen)_3^{2+}$ in the presence or absence of TFA, c[$Os(phen)_3^{2+}$] = 1×10^{-5} M, 1,2-dichloroethane as solvent.

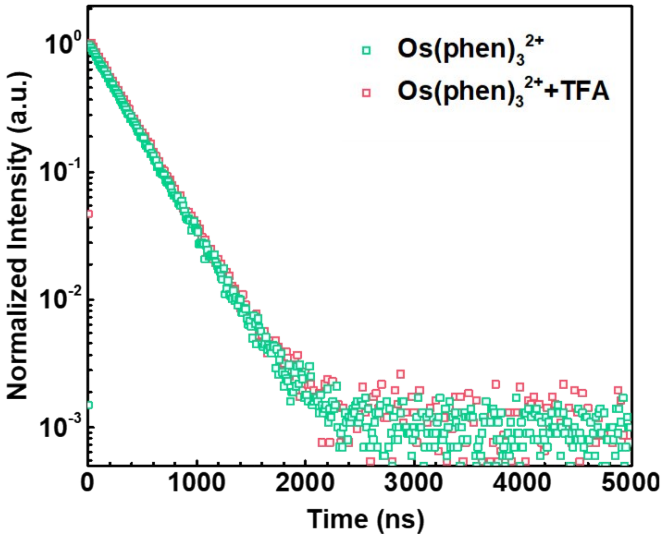

Figure S14. The transient photoluminescence decay curves of $Os(phen)_3^{2+}$ in presence or absence of TFA. λ_{ex} = 640 nm. c[$Os(phen)_3^{2+}$] = 1×10^{-5} M, 1,2-dichloroethane as solvent.

8. The time-dependent absorption spectra of hemiindigo

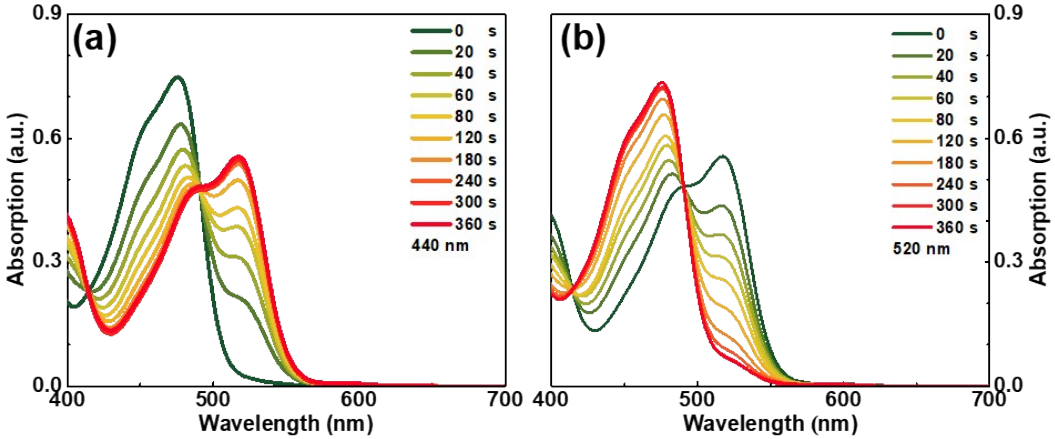

Figure S15. The time-dependent absorption spectra of hemiindigo in toluene solution under photoexcitation at 440 nm (a) and 520 nm (b), c[hemiindigo]= 3×10^{-5} M. The power density of Xenon lamp = 67 mW•cm^{-2} (440 nm), 45 mW•cm^{-2} (520 nm).

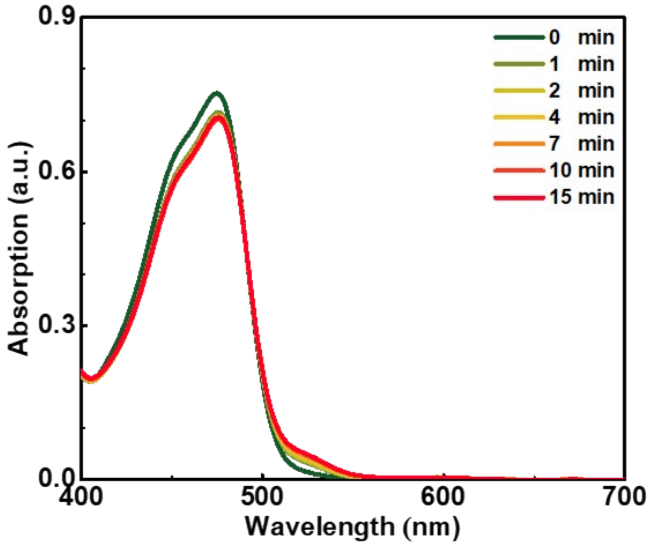

Figure S16. The time-dependent absorption spectra of hemiindigo in toluene solution under photoexcitation at 638 nm, c[hemiindigos]= 3×10^{-5} M.

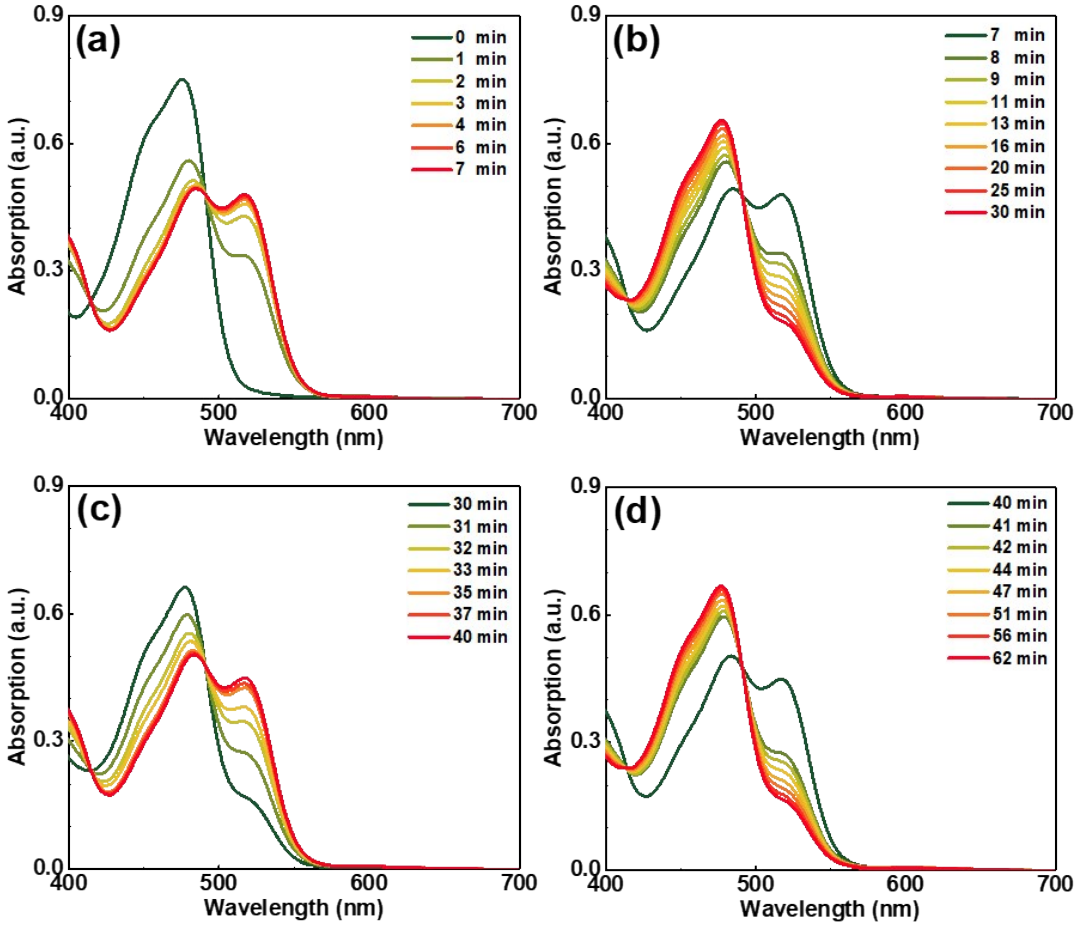

Figure S17. Time-dependent absorption spectra of hemiindigos with TTA-UC fluorescence as excitation light source, c[hemiindigo]= 3×10^{-5} M, toluene as solvent. The reversibility of the acid-base switching of upconversion emission under photoexcitation at 638 nm. (a) In absence of acid-base; (b) with addition of TFA; (c) with addition of TEA; (d) with addition of TFA. 1,2-dichloroethane as the solvent, c[$Os(phen)_3^{2+}$] = 1×10^{-5} M, c[DPyA]=5 mM, λ_{ex} = 638 nm.

9. Calculated the ratio of Z and E isomer of hemiindigo

According to the previous work,[3] the absorption peaks of *Z* isomer and *E* isomer are 476 nm and 518 nm, and the molar extinction coefficient are shown in Table S1.

Table S1. The molar extinction coefficient of *Z* and *E* isomer of hemiindigo

Peak / nm	*Z* isomer / M^{-1}•cm^{-1}	*E* isomer / M^{-1}•cm^{-1}
476	25847	12299
518	519	20358

Based on the absorption spectra, the conversion ratio between *Z* isomer and *E* isomer of hemiindigo under UC irradiation could be deduced by the equation S3 and S4.

$$\varepsilon_{476\,nm} = 25847 \times \Phi_Z + 12299 \times \Phi_E \qquad \text{(S3)}$$

$$\varepsilon_{518\,nm} = 519 \times \Phi_Z + 20358 \times \Phi_E \qquad \text{(S4)}$$

Where $\varepsilon_{476\,nm}$ and $\varepsilon_{518\,nm}$ are the molar extinction coefficients of hemiindigo at 476 nm and 518 nm; Φ_Z and Φ_E are the percentage of *Z* isomer and *E* isomer of hemiindigo after irradiation, respectively.

References

[1] Y. Wei, M. Zheng, L. Chen, X. Zhou and S. Liu, *Dalton Trans.*, 2019, **48**, 11763-11771.

[2] Y. Wei, Y. Li, M. Zheng, X. Zhou, Y. Zou and C. Yang, *Adv. Opt. Mater.*, 2020, **8**, 1902157.

[3] C. Petermayer, S. Thumser, F. Kink, P. Mayer and H. Dube, *J. Am. Chem. Soc.*, 2017, **139**, 15060-15067.